Form-factor-independent test of lepton universality in semileptonic heavy meson and baryon decays

Stefan Groote[,1,*] Mikhail A. Ivanov[,2,†] Jürgen G. Körner[,3,‡] Valery E. Lyubovitskij[,4,5,6,7,§]
Pietro Santorelli[,8,9,‖] and Chien-Thang Tran[8,9,10,¶]

[1]*Füüsika Instituut, Tartu Ülikool, W. Ostwaldi 1, EE-50411 Tartu, Estonia*
[2]*Bogoliubov Laboratory of Theoretical Physics, Joint Institute for Nuclear Research,
141980 Dubna, Russia*
[3]*PRISMA+ Cluster of Excellence, Institut für Physik, Johannes Gutenberg-Universität,
D-55099 Mainz, Germany*
[4]*Institut für Theoretische Physik, Universität Tübingen, Kepler Center for Astro and Particle Physics,
Auf der Morgenstelle 14, D-72076 Tübingen, Germany*
[5]*Departamento de Física y Centro Científico Tecnológico de Valparaíso-CCTVal,
Universidad Técnica Federico Santa María, Casilla 110-V, Valparaíso, Chile*
[6]*Department of Physics, Tomsk State University, 634050 Tomsk, Russia*
[7]*Tomsk Polytechnic University, 634050 Tomsk, Russia*
[8]*Dipartimento di Fisica "E. Pancini," Università di Napoli Federico II, Complesso Universitario di Monte
S. Angelo, Via Cintia, Edificio 6, 80126 Napoli, Italy*
[9]*Istituto Nazionale di Fisica Nucleare, Sezione di Napoli, 80126 Napoli, Italy*
[10]*Department of Physics, Faculty of Applied Sciences, HCMC University of Technology and Education,
Vo Van Ngan 1, Thu Duc, Ho Chi Minh City, Vietnam*

In the semileptonic decays of heavy mesons and baryons, the lepton-mass dependence factors out in the quadratic $\cos^2\theta$ coefficient of the differential $\cos\theta$ distribution. We call the corresponding normalized coefficient the convexity parameter. This observation opens the path to a test of lepton universality in semileptonic heavy meson and baryon decays that is independent of form-factor effects. By projecting out the quadratic rate coefficient, dividing out the lepton-mass-dependent factor, and restricting the phase space integration to the τ lepton phase space, one can define optimized partial rates which, in the Standard Model, are the same for all three (e, μ, τ) modes in a given semileptonic decay process. We discuss how the identity is spoiled by new physics effects. We discuss semileptonic heavy meson decays such as $\bar{B}^0 \to D^{(*)+}\ell^-\bar{\nu}_\ell$ and $B_c^- \to J/\psi(\eta_c)\ell^-\bar{\nu}_\ell$ and semileptonic heavy baryon decays such as $\Lambda_b \to \Lambda_c\ell^-\bar{\nu}_\ell$ for each $\ell = e, \mu, \tau$.

I. INTRODUCTION

Recently, there has been an extraordinary amount of experimental and theoretical activity on the analysis of semileptonic heavy meson and baryon decays. The semileptonic decays $B \to D^{(*)} + \ell\bar{\nu}_\ell$ ($D^{(*)} = D$ or D^*, $\ell = e$, μ, τ) are the best-studied processes. Starting with the

*stefan.groote@ut.ee
†ivanovm@theor.jinr.ru
‡jukoerne@uni-mainz.de
§valeri.lyubovitskij@uni-tuebingen.de
‖Pietro.Santorelli@na.infn.it
¶thangtc@hcmute.edu.vn

BABAR papers [1,2], this upsurge of activity has been fueled by possible observations of the violation of lepton flavor universality which, if true, would signal possible new physics (NP) contributions in these decays. The decays $B \to D^{(*)} + \tau\bar{\nu}_\tau$ have been also studied by the Belle [3–6] and LHCb [7] experiments. The present situation concerning the so-called flavor anomalies is summarized in Refs. [8–11].

The present tests of lepton flavor universality suffer from their dependence on the assumed form of the q^2 behavior of the transition form factors. In the Standard Model (SM), the three semileptonic $(\ell = e, \mu, \tau)$ modes of a given decay are governed by the same set of form factors. However, due to the kinematical constraint $m_\ell^2 \leq q^2 \leq (m_1 - m_2)^2$, the form factors are probed in different regions of q^2. Furthermore, the helicity flip factor $\delta_\ell = m_\ell^2/2q^2$ multiplying the helicity flip contributions provides an additional weight factor depending on q^2 and the lepton mass, which differ for the

three modes. All in all, the tests of lepton universality based on rate measurements alone suffer from a complex interplay of the above two effects which is difficult to control. Ultimately, such tests require the exact knowledge of the q^2 behavior of the various transition form factors, which is difficult to obtain with certainty (see, e.g., Ref. [12]). Instead, one would prefer tests of lepton universality which are independent of form-factor effects such as we are proposing in this paper.

It turns out that the above two obstacles to a clean test of lepton universality can be overcome by (i) restricting the analysis to the phase space of the τ mode and (ii) choosing angular observables for which the helicity flip contributions can be factored out. Fortunately, such an observable is provided by the coefficient of the $\cos^2\theta$ contribution in the differential $\cos\theta$ distribution.

The restriction to a reduced phase space will lead to a loss in rate for the $\ell = \mu, e$ modes which will hopefully be compensated by the 40-fold increase in luminosity provided by the SuperKEKb accelerator at the Belle II detector. For example, the loss in rate through the phase space reduction $(\Gamma_{\text{tot}} - \Gamma_{\text{red}})/\Gamma_{\text{tot}}$ is given by $\mathcal{O}(50)\%$ and $\mathcal{O}(30)\%$ for the decays $\bar{B}^0 \to D^+\ell^-\bar{\nu}_\ell$ and $\bar{B}^0 \to D^{*+}\ell^-\bar{\nu}_\ell$ ($\ell = e, \mu$), respectively. Much more demanding in terms of experimental accuracy is the fact that the proposed test requires an angular analysis which is not mandatory in those tests using the rate alone.

The proposed test of lepton universality will lead to the SM equality of certain optimized ("optd") rates $\Gamma_{U-2L}^{\text{optd}}$ in the three (e, μ, τ) modes; i.e., one has

$$\Gamma_{U-2L}^{\text{optd}}(e) = \Gamma_{U-2L}^{\text{optd}}(\mu) = \Gamma_{U-2L}^{\text{optd}}(\tau). \tag{1}$$

While the actual values of the optimized rates in Eq. (1) are form-factor dependent, the unit ratio of any of the two optimized rates in Eq. (1) or, equivalently, the ratio of the corresponding branching fractions is form-factor independent; i.e., one has

$$R^{\text{optd}}(\ell, \ell') = \frac{\Gamma_{U-2L}^{\text{optd}}(\ell)}{\Gamma_{U-2L}^{\text{optd}}(\ell')} = \frac{B_{U-2L}^{\text{optd}}(\ell)}{B_{U-2L}^{\text{optd}}(\ell')} = 1. \tag{2}$$

In this way, one can test μ/e, τ/μ, and τ/e lepton universality regardless of form-factor effects. NP contributions designed to strengthen the τ rate will clearly lead to a violation of the equalities (1) or the unit ratio of optimized rates (2). The size of the NP violations can be used to constrain the parameter space of the NP contributions in a model-dependent way.

II. GENERIC DIFFERENTIAL $\cos\theta$ DISTRIBUTION

We discuss three kinds of semileptonic heavy hadron decays involving the $b \to c$ current transition, namely,

the decays $P(0^-) \to P'(0^-)\ell\bar{\nu}$, $P(0^-) \to V(1^-)\ell\bar{\nu}$, and $B(1/2^+) \to B'(1/2^+)\ell\bar{\nu}$. We expand the generic differential $(q^2, \cos\theta)$ distribution for these decays in terms of their helicity structure functions [13–20]

$$\frac{d^2\Gamma}{dq^2 d\cos\theta} = \frac{2}{2S_1 + 1}\frac{3}{8}\frac{\Gamma_0|\vec{q}|q^2 v^2}{m_1^7} \times (A_0 + A_1\cos\theta + A_2\cos^2\theta), \tag{3}$$

where S_1 is the spin of the initial hadron and

$$\Gamma_0 = \frac{G_F^2|V_{cb}|^2 m_1^5}{192\pi^3} \tag{4}$$

is the fundamental rate occurring in the weak three-body decay transitions of particle with mass m_1 and governed by the weak coupling $G_F|V_{cb}|$. The momentum transfer is denoted by $q = p_1 - p_2$, and $|\vec{q}| = |\vec{p}_2| = \sqrt{Q_+Q_-}/2m_1$ is the momentum of the daughter particle in the rest system of the parent particle with $Q_\pm = (m_1 \pm m_2)^2 - q^2$. The polar angle of the charged lepton in the (l, ν_l) c.m. system relative to the momentum direction of the $W_{\text{off-shell}}$ is denoted by θ.

The coefficients A_0, A_1, and A_2 are given, respectively, by

$$A_0 = \mathcal{H}_U + 2\mathcal{H}_L + 2\delta_\ell(\mathcal{H}_U + 2\mathcal{H}_S), \tag{5}$$

$$A_1 = -2(\mathcal{H}_P + 4\delta_\ell\mathcal{H}_{SL}), \tag{6}$$

$$A_2 = v(\mathcal{H}_U - 2\mathcal{H}_L). \tag{7}$$

In Eq. (6), we have introduced the velocity-type parameter $v = 1 - m_\ell^2/q^2$ which, when expressed in terms of the helicity flip factor $\delta_\ell = m_\ell^2/2q^2$, reads $v = 1-2\delta_\ell$. The helicity structure functions $\mathcal{H}_X(X = U, L, \dots)$ are bilinear combinations of the helicity amplitudes which will be specified later on. Note that the coefficient A_2 factors into the q^2- and lepton-mass-dependent factor $v = 1 - m_\ell^2/q^2$ and the q^2-dependent combination $\mathcal{H}_U(q^2) - 2\mathcal{H}_L(q^2)$. We mention that, instead of expanding the $(q^2, \cos\theta)$ distribution in terms of helicity structure functions as in Eq. (3), one can also expand the decay distribution in terms of invariant structure functions [21–24].

The cosine of the polar angle θ can be related to the energy E_ℓ of the lepton measured in the rest system of the parent particle. The relation reads (see, e.g., [13,16])

$$\cos\theta = \frac{2E_\ell - q_0(1 + 2\delta_\ell)}{|\vec{q}|v} \tag{8}$$

with $-1 \leq \cos\theta \leq 1$. The energy of the off-shell W boson in the rest system of the parent particle is given by

$$q_0 = (m_1^2 - m_2^2 + q^2)/(2m_1). \qquad (9)$$

For our purposes, it is more convenient to rewrite the $\cos\theta$ distribution in terms of the Legendre polynomials. One of the advantages of the Legendre representation is that one can project out the coefficient A_2 in a straightforward way. One has

$$\frac{d^2\Gamma}{dq^2 d\cos\theta} = \frac{1}{2S_1 + 1} \frac{\Gamma_0 |\vec{q}| q^2 v^2}{m_1^7} \{\mathcal{H}_{\text{tot}}(q^2, m_\ell^2) P_0(\cos\theta)$$
$$+ \mathcal{H}_1(q^2, m_\ell^2) P_1(\cos\theta) + v\mathcal{H}_2(q^2) P_2(\cos\theta)\}. \qquad (10)$$

The coefficient functions $\mathcal{H}_{\text{tot}}$, $\mathcal{H}_1$, and $\mathcal{H}_2$ are given, respectively, by

$$\mathcal{H}_{\text{tot}}(q^2, m_\ell^2) = (1 + \delta_\ell)(\mathcal{H}_U + \mathcal{H}_L) + 3\delta_\ell \mathcal{H}_S,$$
$$\mathcal{H}_1(q^2, m_\ell^2) = -\frac{3}{2}(\mathcal{H}_P + 4\delta_\ell \mathcal{H}_{SL}),$$
$$\mathcal{H}_2(q^2) = \frac{1}{2}(\mathcal{H}_U - 2\mathcal{H}_L) = \frac{1}{2}\mathcal{H}_{U-2L}. \qquad (11)$$

For the convenience of the reader, we list some properties of the Legendre polynomials:

$$P_0(\cos\theta) = 1, \qquad P_1(\cos\theta) = \cos\theta,$$
$$P_2(\cos\theta) = \frac{1}{2}(3\cos^2\theta - 1). \qquad (12)$$

The Legendre polynomials satisfy the orthonormality relation

$$\int_{-1}^{+1} dx P_m(x) P_n(x) = \frac{2}{2n+1}\delta_{mn}. \qquad (13)$$

It is now straightforward to extract the observables $\mathcal{H}_{\text{tot}}$, $\mathcal{H}_1$, and $\mathcal{H}_2$ from Eq. (10) by folding the angular distribution with the relevant Legendre polynomial. For instance, the differential decay rate is obtained by folding in $P_0(\cos\theta)$ as follows:

$$\frac{d\Gamma}{dq^2} = \int_{-1}^{1} d\cos\theta \frac{d^2\Gamma}{dq^2 d\cos\theta} P_0(\cos\theta)$$
$$= \frac{2}{2S_1 + 1} \frac{\Gamma_0 |\vec{q}| q^2 v^2}{m_1^7} \mathcal{H}_{\text{tot}}(q^2, m_\ell^2). \qquad (14)$$

The partial differential rate $d\Gamma_{U-2L}/dq^2$ can be projected out by folding in $P_2(\cos\theta)$ according to

$$\frac{d\Gamma_{U-2L}}{dq^2} = 10 \int_{-1}^{1} d\cos\theta \frac{d^2\Gamma}{dq^2 d\cos\theta} P_2(\cos\theta)$$
$$= \frac{2}{2S_1 + 1} \frac{\Gamma_0 |\vec{q}| q^2 v^3}{m_1^7} \mathcal{H}_{U-2L}(q^2), \qquad (15)$$

where the helicity structure function $\mathcal{H}_{U-2L}(q^2)$ defined in Eq. (11) is a function of q^2 only (see also Refs. [22–24]). The overall factor 10 in Eq. (15) has been chosen such to have the same normalization of Eqs. (14) and (15).

In Refs. [17,18], we have defined a convexity parameter $C_F(q^2, \ell)$ as a measure of the curvature of the $\cos\theta$ distribution by taking the second derivative of the $\cos\theta$ distribution. The relation of the convexity parameter to the ratio of the two differential rates (14) and (15) is given by

$$C_F(q^2, \ell) = \frac{3}{4} \frac{d\Gamma_{U-2L}(q^2, \ell)/dq^2}{d\Gamma(q^2, \ell)/dq^2}. \qquad (16)$$

Also, we introduce the average values of the convexity parameter $\langle C_F^\ell \rangle$ where the average is taken in the interval $m_\tau^2 \leq q^2 \leq (m_1 - m_2)^2$ for both μ and τ modes:

$$\langle C_F^\ell \rangle = \frac{3}{4} \frac{\int_{m_\tau^2}^{(m_1-m_2)^2} dq^2 d\Gamma_{U-2L}(q^2, \ell)/dq^2}{\int_{m_\tau^2}^{(m_1-m_2)^2} dq^2 d\Gamma(q^2, \ell)/dq^2}, \qquad \ell = \mu, \tau.$$
$$(17)$$

An interesting method to compare the theoretical prediction for the angular observables like the convexity parameter with experimental data was proposed in Ref. [25]. It is based on counting the number of events in certain regions of the Dalitz plot.

III. OPTIMIZED OBSERVABLES

The possible breaking of lepton flavor universality is usually studied by analyzing the ratios of rates or, equivalently, the ratio of branching ratios for the tau and muon modes. As discussed in the introduction, one can remove the lepton-mass effects by introducing two improvements. First, we propose to analyze observables in the common phase space region $m_\tau^2 \leq q^2 \leq (m_1 - m_2)^2$ as has been suggested before in Refs. [26–28]. As an example, in Fig. 1, we show the $(q^2, \cos\theta)$ phase space for the decay
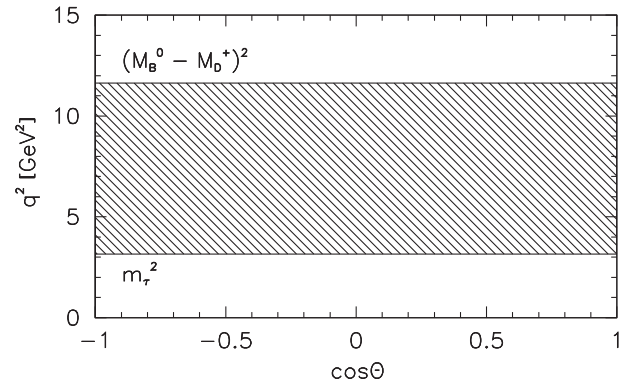

FIG. 1. $(q^2, \cos\theta)$ phase space for $\bar{B}^0 \to D^+ + \ell^- + \bar{\nu}_\ell$. The hatched region shows the $\ell = \tau$ phase space.

$\bar{B}^0 \to D^+ + \ell^- + \bar{\nu}_\ell$, where the hatched area shows the common phase space region $m_\tau^2 \leq q^2 \leq (m_1 - m_2)^2$. Second, we reweigh suitable observables in which the lepton-mass dependence factors out by dropping the overall lepton-mass-dependent factor. As Eqs. (3) and (10) show, such an observable is available through the coefficient of the quadratic $\cos^2 \theta$ term in the angular decay distribution proportional to the helicity structure function $v \mathcal{H}_{U-2L}$.

Based on Eq. (15), we define an optimized differential partial rate by dividing out the factor v^3. One has

$$\frac{d\Gamma_{U-2L}^{\text{optd}}(q^2, \ell)}{dq^2} = v^{-3} \frac{d\Gamma_{U-2L}(q^2, \ell)}{dq^2}$$
$$= \frac{2\Gamma_0}{2S_1 + 1} \frac{|\vec{q}|q^2}{m_1^7} \mathcal{H}_{U-2L}(q^2), \quad (18)$$

which by construction does not depend on the lepton mass. In terms of the ratios of branching fractions

$$B_{U-2L}^{\text{optd}}(q^2, \ell) = \tau \frac{d\Gamma_{U-2L}^{\text{optd}}(q^2, \ell)}{dq^2}, \quad (19)$$

where τ is the lifetime of the respective hadron, Eq. (18) leads to

$$R_{U-2L}^{\text{optd}}(q^2; \ell, \ell') = \frac{B_{U-2L}^{\text{optd}}(q^2, \ell)}{B_{U-2L}^{\text{optd}}(q^2, \ell')} = 1. \quad (20)$$

Equation (20) can be used to test lepton universality on the differential q^2 level by analyzing the ratios of the optimized branching fractions $R_{U-2L}^{\text{optd}}(q^2; \tau, \mu) = R_{U-2L}^{\text{optd}}(q^2; \tau, e) = R_{U-2L}^{\text{optd}}(q^2; \mu, e)$ in the reduced phase space region $m_\tau^2 \leq q^2 \leq q_{\max}^2$. In practice, one would lump the light lepton modes together and concentrate on the ratio of branching fractions $R_{U-2L}^{\text{optd}}(q^2; \tau, (\mu + e)) = 1/2$.

After q^2 integration over the reduced phase space region, one has

$$\Gamma_{U-2L}^{\text{optd}}(\ell) = \int_{m_\tau^2}^{(m_1 - m_2)^2} dq^2 \frac{d\Gamma_{U-2L}^{\text{optd}}(q^2, \ell)}{dq^2}. \quad (21)$$

The proposed test of lepton universality will lead to the equality of the optimized partial rates $\Gamma_{U-2L}^{\text{optd}}(\ell)$ in the three (e, μ, τ) modes:

$$\Gamma_{U-2L}^{\text{optd}}(e) = \Gamma_{U-2L}^{\text{optd}}(\mu) = \Gamma_{U-2L}^{\text{optd}}(\tau) \quad (22)$$

or, equivalently, to the equality of the three corresponding optimized branching ratios:

$$B_{U-2L}^{\text{optd}}(e) = B_{U-2L}^{\text{optd}}(\mu) = B_{U-2L}^{\text{optd}}(\tau). \quad (23)$$

The equality of the three optimized rates or optimized branching ratios is independent of form-factor effects, while the actual value of the optimized rates or optimized branching ratios is form-factor dependent and is, thus, model dependent. However, the ratio of the (e, μ, τ) branching fractions is predicted to be equal to one, independently of form-factor effects; i.e., one has

$$R_{U-2L}^{\text{optd}}(\ell, \ell') = \frac{B_{U-2L}^{\text{optd}}(\ell)}{B_{U-2L}^{\text{optd}}(\ell')} = 1. \quad (24)$$

Since the $(q^2, \cos \theta)$ phase space is rectangular, the q^2 and $\cos \theta$ integrations can be interchanged. One can, therefore, first integrate over q^2 and then do the $U - 2L$ projection rather than first projecting out $\mathcal{H}_{U-2L}$ and then doing the q^2 integration. This may be of advantage in the experimental analysis.

Note that our definition of the optimized rates or branching ratios differs from the one used in Ref. [28]. In order to differentiate between the two definitions, we denote our optimized rates by the label "optd" instead of the label "opt" used in Ref. [28]. The authors of Ref. [28] define an optimized rate ratio

$$R^{\text{opt}} = \frac{\int_{m_\tau^2}^{(m_1 - m_2)^2} d\Gamma^{\text{opt}}(\tau)/dq^2}{\int_{m_\tau^2}^{(m_1 - m_2)^2} (1 - 2\delta_\tau)^2(1 + \delta_\tau) d\Gamma^{\text{opt}}(\mu)/dq^2} > 1. \quad (25)$$

The numerator exceeds the denominator because of the addition of a definitely positive scalar contribution in the numerator.

The idea behind the definition (25) is to define an R measure R^{opt} which minimizes the propagation of form-factor errors to the optimized R measure R^{opt}. This goal is, in fact, achieved by the R measure R^{opt} (25) as shown in Ref. [28].

IV. THREE CLASSES OF SEMILEPTONIC DECAYS

We now discuss three classes of prominent $b \to c$-induced semileptonic decays in turn. We begin with the decay $P(0^-) \to P'(0^-)\ell\bar{\nu}_\ell$.

A. $P(0^-) \to P'(0^-)\ell\bar{\nu}_\ell$ decay

The decays $\bar{B}^0 \to D^+\ell^-\bar{\nu}_\ell$ and $B_c^+ \to \eta_c\ell^+\nu_\ell$ belong to this class of decays. The two form factors describing the $B \to D$ transition are defined by (see, e.g., Refs. [13,18])

$$\langle P_2|J_\mu^V|P_1\rangle = F_+(q^2)(p_1 + p_2)_\mu + F_-(q^2)q_\mu. \quad (26)$$

The corresponding helicity amplitudes H_{λ_W} read

$$H_0 = \frac{2m_1|\vec{q}|}{\sqrt{q^2}} F_+(q^2), \qquad H_\pm = 0,$$

$$H_t = \frac{1}{\sqrt{q^2}} (m_+ m_- F_+(q^2) + q^2 F_-(q^2)), \qquad (27)$$

where $m_\pm = m_1 \pm m_2$.

The longitudinal and scalar helicity structure functions are given in terms of the bilinear combinations

$$\mathcal{H}_L = |H_0|^2, \quad \mathcal{H}_U = |H_+|^2 + |H_-|^2 = 0, \quad \mathcal{H}_S = |H_t|^2. \tag{28}$$

Note that the longitudinal structure function $\mathcal{H}_L$ is proportional to $|\vec{q}|^2$. Since the unpolarized transverse structure function $\mathcal{H}_U$ is zero, one has $\mathcal{H}_{U-2L} \sim |\vec{q}|^2$.

B. $P(0^-) \to V(1^-)\ell\bar{\nu}_\ell$ decay

Interesting decays in this class are $\bar{B}^0 \to D^{*+}\ell^-\bar{\nu}_\ell$ and $B_c^- \to J/\Psi\ell^-\bar{\nu}_\ell$. We define invariant form factors according to the expansion (see, e.g., Refs. [13,18])

$$\langle V_2|J_\mu^{V-A}|P_1\rangle = \frac{\epsilon^{\dagger\alpha}}{m_+}(-g_{\mu\alpha}Pq A_0(q^2) + P_\mu P_\alpha A_+(q^2) + q_\mu P_\alpha A_-(q^2) + i\varepsilon_{\mu\alpha Pq}V(q^2)). \tag{29}$$

One has to specify the helicity amplitudes $H_{\lambda_W\lambda_V}$ by the two helicities λ_W and λ_V of the off-shell W boson and the daughter vector meson. The helicity amplitudes are given by

$$H_{t0} = \frac{m_1 m_- |\vec{q}|}{m_2\sqrt{q^2}}\left(-A_0 + A_+ + \frac{q^2}{m_+ m_-}A_-\right),$$

$$H_{\pm1\pm1} = m_-\left(-A_0 \pm \frac{2m_1}{m_+ m_-}|\vec{q}|V\right),$$

$$H_{00} = \frac{m_-}{2m_2\sqrt{q^2}}\left(-(m_+ m_- - q^2)A_0 + \frac{4m_1^2}{m_+ m_-}|\vec{q}|^2 A_+\right). \tag{30}$$

The helicity structure functions read

$$\mathcal{H}_U = |H_{+1+1}|^2 + |H_{-1-1}|^2, \qquad \mathcal{H}_L = |H_{00}|^2,$$
$$\mathcal{H}_S = |H_{t0}|^2. \tag{31}$$

Note that $\mathcal{H}_S, \mathcal{H}_{U-2L} \sim |\vec{q}|^2$. This scaling is obvious for $\mathcal{H}_S$. In the case of $\mathcal{H}_{U-2L}$, it requires a little algebra based on the use of the identity:

$$|\vec{q}|^2 = \frac{(m_+ m_- - q^2)^2}{4m_1^2} - \frac{m_2^2}{m_1^2}q^2. \tag{32}$$

C. $B(\frac{1}{2}^+) \to B'(\frac{1}{2}^+)\ell\bar{\nu}_\ell$ decay

One defines the invariant form factors by writing (see, e.g., Refs. [17,19])

$$\langle B_2|J_\mu^{V/A}|B_1\rangle = \bar{u}_p(p_2)\left[F_1^{V/A}(q^2)\gamma_\mu - i\frac{F_2^{V/A}(q^2)}{m_1}\sigma_{\mu\nu}q^\nu + \frac{F_3^{V/A}(q^2)}{m_1}q_\mu\right](I/\gamma_5)u_n(p_1). \tag{33}$$

The corresponding helicity amplitudes $H_{\lambda_2\lambda_W}^{V/A}$ read

$$H_{\frac{1}{2}t}^{V/A} = \frac{\sqrt{Q_\pm}}{\sqrt{q^2}}\left(m_\mp F_1^{V/A}(q^2) \pm \frac{q^2}{m_1}F_3^{V/A}(q^2)\right),$$

$$H_{\frac{1}{2}0}^{V/A} = \frac{\sqrt{Q_\mp}}{\sqrt{q^2}}\left(m_\pm F_1^{V/A}(q^2) \pm \frac{q^2}{m_1}F_2^{V/A}(q^2)\right),$$

$$H_{\frac{1}{2}1}^{V/A} = \sqrt{2Q_\mp}\left(F_1^{V/A}(q^2) \pm \frac{m_\pm}{m_1}F_2^{V/A}(q^2)\right). \tag{34}$$

From parity or from an explicit calculation, one has $H_{-\lambda_2-\lambda_W}^V = +H_{\lambda_2\lambda_W}^V$ and $H_{-\lambda_2-\lambda_W}^A = -H_{\lambda_2\lambda_W}^A$. The relevant helicity structure functions read

$$\mathcal{H}_U = 2\left(|H_{+\frac{1}{2}+1}^V|^2 + |H_{+\frac{1}{2}+1}^A|^2\right),$$

$$\mathcal{H}_L = 2\left(|H_{+\frac{1}{2}0}^V|^2 + |H_{+\frac{1}{2}0}^A|^2\right),$$

$$\mathcal{H}_S = 2\left(|H_{+\frac{1}{2}t}^V|^2 + |H_{+\frac{1}{2}t}^A|^2\right). \tag{35}$$

With a little algebra, one finds $\mathcal{H}_{U-2L} \sim |\vec{q}|^2$.

In all three classes of decays, one finds that the helicity structure function combination $\mathcal{H}_{U-2L} = \mathcal{H}_U - 2\mathcal{H}_L$ is proportional to $|\vec{q}|^2$. This leads to a depletion of the partial rate $d\Gamma_{U-2L}^{opt}/dq^2$ close to the zero recoil $q^2 = (m_1 - m_2)^2$, where $|\vec{q}| = 0$. In this paper, we do not study the parity-odd helicity structure functions $\mathcal{H}_P$ and $\mathcal{H}_{SL}$, which scale as $\mathcal{H}_P, \mathcal{H}_{SL} \sim |\vec{q}|$ [16–19].

V. NUMERICAL RESULTS

We are now in the position to discuss the numerical values for the optimized observables introduced in our paper. The key point here is the choice of the form factors characterizing the $B \to D^{(*)}$ and $\Lambda_b \to \Lambda_c$ transitions. In addition to various model calculations, there are precise lattice QCD determinations for these form factors. The first lattice-QCD determination of the form factors describing the semileptonic decays $\Lambda_b \to \Lambda_c^{(*)} + \ell\bar{\nu}_\ell$ has been performed in Refs. [29–31]. The Fermilab Lattice and MILC Collaborations have presented the computations of zero-recoil form factor for $B \to D^{(*)} + \ell\bar{\nu}_\ell$ decay in Ref. [32]

and unquenched lattice-QCD calculation of the hadronic form factors for the exclusive decay $B \to D + \ell \bar{\nu}_\ell$ at nonzero recoil in Ref. [33]. In Ref. [34], the HPQCD Collaboration has presented a lattice QCD calculation of the $B \to D + \ell \bar{\nu}_\ell$ decay for the entire physical q^2 range. The branching fraction ratio was found to be $R(D) = 0.300(8)$. The $B - D$ calculations in particular are precise, cover various q^2 values, and have been combined with experimental data for the light lepton q^2 distribution to cover the full spectrum. Something similar has been done with $B - D^*$ as well; see Refs. [35–38]. The lattice determinations of the form factors were also employed to extract the value of V_{cb}. The numerical values for the optimized observables introduced in this paper are calculated by using the form factors obtained in the framework of the covariant confined quark model (CCQM). The behavior of all CCQM form factors was found to be quite smooth in the full kinematical range of the semileptonic transitions. In fact, they are well represented by a two-parameter representation in terms of a double-pole parametrization:

$$F(q^2) = \frac{F(0)}{1 - as + bs^2}, \qquad s = \frac{q^2}{m_1^2}. \qquad (36)$$

The values of the fitted parameters a, b, and $F(q^2 = 0)$ are listed in Eq. (34) of Ref. [18] for the $B \to D^{(*)}$ transition, in Table I of Ref. [39] for the $B_c \to \eta_c$ and $B_c \to J/\psi$ transitions, and in Eq. (59) of Ref. [17] for the $\Lambda_b \to \Lambda_c$ transition. The values of the lepton and hadron masses and their lifetimes as well as the value of the Cabibbo-Kobayashi-Maskawa matrix element V_{cb} are taken from the PDG [40].

In Table I, we list the average values of the convexity $\langle C_F^\ell \rangle$. For the two transitions $B \to D$ and $B_c \to \eta_c$, we get $\langle C_F^\mu \rangle = -1.49 \simeq -3/2$ in the μ mode. The reason for such a common value in both transitions is that there is no transverse contribution in the $P \to P'$ transitions and the muon mass is strongly suppressed in comparison with the τ lepton mass $(m_\mu/m_\tau \ll 1)$. In the limit $m_\mu/m_\tau \equiv 0$, one gets $\langle C_F^\mu \rangle \equiv -3/2$. In case of the τ mode for the two $P \to P'$ transitions, the average convexity parameter is quite small: -0.26 for the $B \to D$ transition and -0.24 for the $B_c \to \eta_c$ transition. Note that the entries in Table I are form-factor dependent. In case of the $P \to V$ transitions, one can see that the average convexity parameter is again

TABLE I. q^2 averages of the convexity parameters $\langle C_F^\mu \rangle$ and $\langle C_F^\tau \rangle$ in the range $m_\tau^2 \le q^2 \le (m_1 - m_2)^2$.

Obs	$B \to D$	$B_c \to \eta_c$	$B \to D^*$	$B_c \to J/\psi$	$\Lambda_b \to \Lambda_c$
$\langle C_F^\mu \rangle$	-1.49	-1.49	-0.27	-0.22	-0.44
$\langle C_F^\tau \rangle$	-0.26	-0.24	-0.062	-0.050	-0.10

suppressed for the τ modes. We also notice that $\langle C_F^\ell \rangle$ is more suppressed for the $P \to V$ transitions in comparison with the $P \to P'$ transitions. Finally, for the $\Lambda_b \to \Lambda_c$ transition, we get the $\langle C_F^\ell \rangle$ parameters, which lie between the ones for the $P \to V$ and $P \to P'$ transitions.

In Fig. 2, we show the behavior of $d\Gamma_{U-2L}^{\text{optd}}/dq^2$ and $d\Gamma_{U-2L}/dq^2 = v^3 d\Gamma_{U-2L}^{\text{optd}}/dq^2$ (τ mode) in the region $m_\tau^2 \le q^2 \le (m_1 - m_2)^2$. In the case of ℓ, μ modes, the two above rates coincide with high accuracy.

The differential rates are largest at threshold $q^2 = m_\tau^2$ and go to zero at the zero-recoil point $q^2 = (m_1 - m_2)^2$ with the characteristic $|\vec{q}|^3$ dependence. The (form-factor-dependent) numerical values of the integrated observables are given in Table II. We also list their average values for the range $4 \text{ GeV}^2 \le q^2 \le (m_1 - m_2)^2$ to highlight the fact that the differential rates are largest in the region close to threshold, where, in the τ mode, the division by v^3 is potentially problematic from the experimental point of view.

Next, we address the question of how to compare the numerical values calculated in Table II with the outcome of the corresponding experimental measurements. We first assume that the number of the produced parent particles is known, which, in the case of produced $\bar{B}^0$'s, we will refer to as $N(\bar{B}^0 \text{tags})$. For example, in $e^+ e^-$ annihilations on the $\Upsilon(4S)$ resonance the bottom mesons are produced in pairs, and the identification of a B^0 on one side can be used as a tag for the $\bar{B}^0$ on the opposite side. In an experimental analysis, one counts the number of events of a given decay and relates this to the known number of produced particles given by $N(\bar{B}^0 \text{tags})$.

One can then define an experimental branching fraction by writing

$$B(\bar{B}^0 \to D^+ \ell^- \bar{\nu}_\ell) = \frac{N(\bar{B}^0 \to D^+ \ell^- \bar{\nu}_\ell)}{N(\bar{B}^0 \text{tags})}, \qquad (37)$$

which can be compared to the theoretical branching fraction

$$B(\bar{B}^0 \to D^+ \ell^- \bar{\nu}_\ell) = \tau(\bar{B}^0) \Gamma_{\text{tot}}(\bar{B}^0 \to D^+ \ell^- \bar{\nu}_\ell). \qquad (38)$$

In the same way, one can define an experimental optimized branching fraction by writing

$$B_{U-2L}^{\text{optd}}(\bar{B}^0 \to D^+ \ell^- \bar{\nu}_\ell) = \frac{N_{U-2L}^{\text{optd}}(\bar{B}^0 \to D^+ \ell^- \bar{\nu}_\ell)}{N(\bar{B}^0 \text{tags})}, \qquad (39)$$

which, again, can be compared to the corresponding theoretical branching fraction

$$B_{U-2L}^{\text{optd}}(\bar{B}^0 \to D^+ \ell^- \bar{\nu}_\ell) = \tau(\bar{B}^0) \Gamma_{U-2L}^{\text{optd}}(\bar{B}^0 \to D^+ \ell^- \bar{\nu}_\ell). \qquad (40)$$
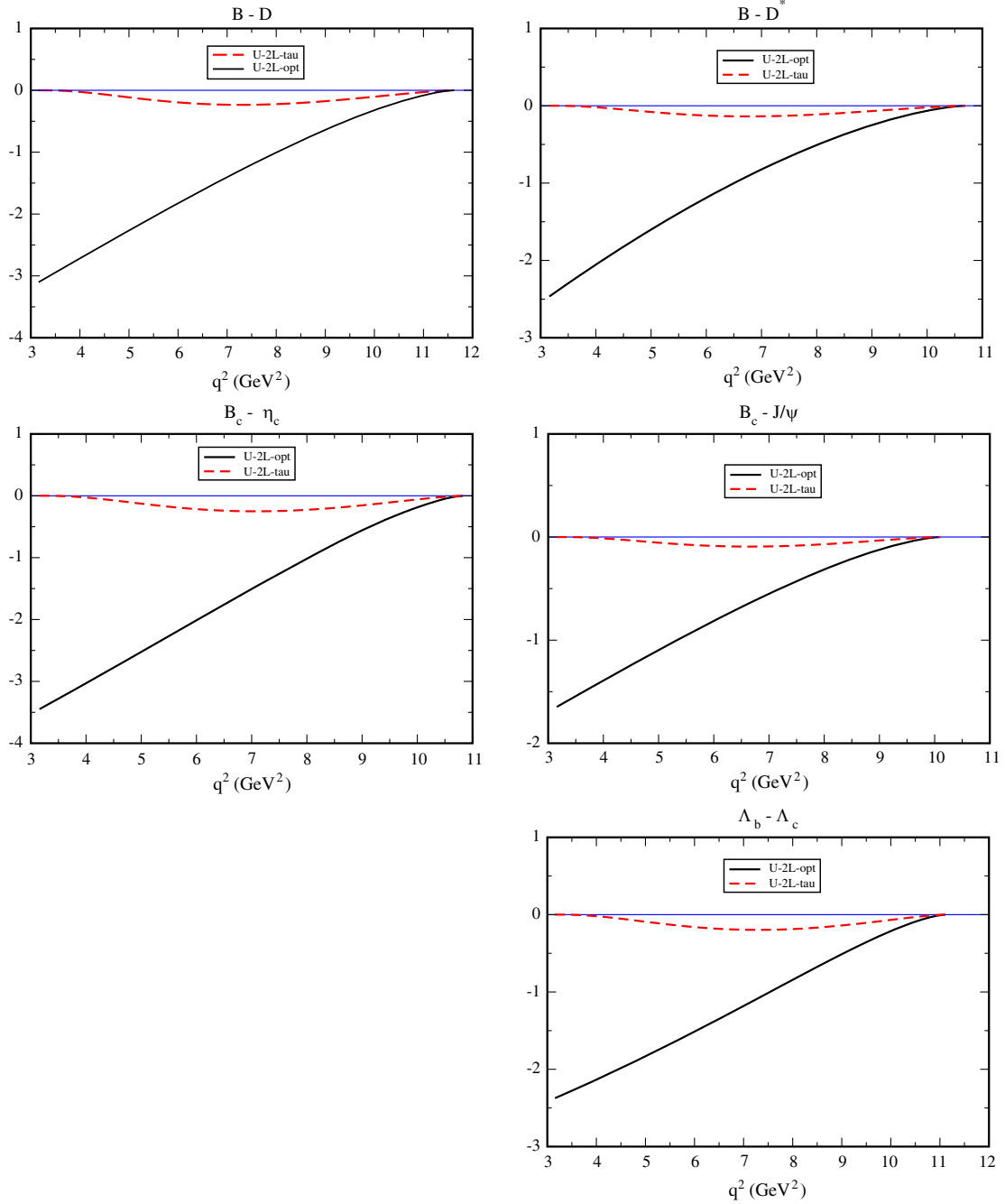
FIG. 2. q^2 dependence of the optimized partial rate $d\Gamma_{U-2L}^{\text{optd}}/dq^2$ (solid curve) and $d\Gamma_{U-2L}/dq^2 = v^3 d\Gamma_{U-2L}^{\text{optd}}/dq^2$ (τ mode, dashed curve) in units of 10^{-15} GeV^{-1}.

One then defines optimized rate ratios $R_{U-L}^{\text{optd}}(\ell, \ell')$ by

$$R_{U-L}^{\text{optd}}(\ell, \ell') = \frac{B_{U-2L}^{\text{optd}}(\ell)}{B_{U-2L}^{\text{optd}}(\ell')} = \frac{N_{U-2L}^{\text{optd}}(\ell)}{N_{U-2L}^{\text{optd}}(\ell')} = \frac{\Gamma_{U-2L}^{\text{optd}}(\ell)}{\Gamma_{U-2L}^{\text{optd}}(\ell')} = 1,$$

(41)

which are predicted to be equal to one.

As the ratios (41) show, tagging is not really required when measuring the optimized rate ratio $R_{U-L}^{\text{optd}}(\ell, \ell')$, since the denominators $N(\bar{B}^0\text{tags})$ drop out when taking the ratio (41). This shows that the optimized rate ratio $R_{U-L}^{\text{optd}}(\ell, \ell')$ can be experimentally determined even for untagged decays as in the B_c^- and Λ_b decays.

TABLE II. The optimized partial rate $\Gamma_{U-2L}^{\text{optd}}$ in units of 10^{-14} GeV.

$q^2_{\min}$	$B \to D$	$B_c \to \eta_c$	$B \to D^*$	$B_c \to J/\psi$	$\Lambda_b - \Lambda_c$
m_τ^2	-1.14	-1.21	-0.73	-0.49	-0.90
4 GeV^2	-0.89	-0.93	-0.54	-0.36	-0.71

VI. NEW PHYSICS CONTRIBUTIONS

At present, $b - c$ transition puzzles motivate many studies of new physics due to the observed deviations from the Standard Model predictions. There are a number of theoretical attempts to resolve these puzzles. See, for example, Refs. [41,42], and other references therein. Possible NP contributions to the semileptonic decays $\bar{B}^0 \to D(D^*)\tau^-\bar{\nu}_\tau$ and $\bar{B}_c \to \eta_c(J/\psi)\tau^-\bar{\nu}_\tau$ have been studied in our papers [39,43,44]. The NP transition form factors have been calculated in the full kinematic q^2 range, employing again the CCQM. The modifications of the partial differential rates $d\Gamma_{U-2L}(\tau)/dq^2$ from the differential $(q^2, \cos\theta)$ distributions of the decays $\bar{B}^0 \to D\tau^-\bar{\nu}_\tau$ and $\bar{B}^0 \to D^*\tau^-\bar{\nu}_\tau$ are presented in Eqs. (14) and (C1), respectively, in Ref. [43]. One has

$$\frac{d\Gamma_{U-2L}(\text{NP})}{dq^2} = \frac{2\Gamma_0}{2S_1+1}\frac{|\vec{q}|q^2}{m_1^7}(1-2\delta_\tau)^3 \mathcal{H}_{U-2L}(\text{NP}),\tag{42}$$

where

$$\mathcal{H}_{U-2L}(\text{NP}) = \begin{cases} -2|1+V_L+V_R|^2|H_0|^2 + 32|T_L|^2|H_T|^2 & (P-P')\text{transition}, \\ (|1+V_L|^2+|V_R|^2)(|H_{++}|^2+|H_{--}|^2-2|H_{00}|^2) \\ -4\text{Re}V_R(H_{++}H_{--}-|H_{00}|^2) \\ -16|T_L|^2(|H_T^+|^2+|H_T^-|^2-2|H_T^0|^2) & (P-V)\text{transition} \end{cases}.$$

If we recall the relations of helicities with the Lorentz form factors, then one gets

$$\mathcal{H}_{U-2L+\text{NP}}^{P-P'} = \frac{4m_1^2|\vec{q}|^2}{q^2}\left\{-2|1+V_L+V_R|^2F_+^2 + 32|T_L|^2\frac{q^2}{m_+^2}F_T^2\right\},$$

$$|H_{++}|^2+|H_{--}|^2-2|H_{00}|^2 = \frac{2m_1^2|\vec{q}|^2}{m_2^2m_+^2q^2}\{-(Pq)^2A_0^2 + 2[2m_2^2q^2V^2 + Pq(Pq-q^2)A_0A_+] - 4m_1^2|\vec{q}|^2A_+^2\},$$

$$H_{++}H_{--}-|H_{00}|^2 = \frac{m_1^2|\vec{q}|^2}{m_2^2m_+^2q^2}\{-(Pq)^2A_0^2 - 2[2m_2^2q^2V^2 - Pq(Pq-q^2)A_0A_+] - 4m_1^2|\vec{q}|^2A_+^2\},$$

$$|H_T^+|^2+|H_T^-|^2-2|H_T^0|^2 = \frac{2m_1^2|\vec{q}|^2}{m_2^2}\left\{\frac{8m_2^2}{q^2}G_1^2 - (G_1+G_2)^2\right.$$
$$\left. + \frac{2}{m_+^2}[(m_1^2+3m_2^2-q^2)G_1 + (Pq-q^2)G_2]G_0 - \frac{4m_1^2|\vec{q}|^2}{m_+^4}G_0^2\right\}.\tag{43}$$

One can see that the differential rate $d\Gamma_{U-2L}$ vanishes as $|\vec{q}|^3$ at zero recoil. Here, $V_{L/R}$ and T_L are the complex Wilson coefficients governing the NP contributions. One has to note that the scalar operators contribute to the full fourfold angular distribution, but they do not appear in the coefficient proportional to $\cos^2\theta$, i.e., in the convexity parameter. It is assumed that NP affects only leptons of the third generation, i.e., the τ lepton mode. Note that the lepton-mass-dependent factor v also factors out in the NP contributions to the $(U - 2L)$ helicity structure function.

The parameters of the dipole approximation for the calculated NP form factors are listed in Eqs. (10) and (11) of Ref. [43] for $B - D$ and $B - D^*$ transitions and in Table I of Ref. [39] for $B_c - \eta_c$ and $B_c - J/\psi$ transitions.

The allowed regions for the NP Wilson coefficients have been found by fitting the experimental data for the ratios $R(D^{(*)})$ by switching on only one of the NP operators at a time.

In each allowed region at 2σ, the best-fit value for each NP coupling was found. The best-fit couplings read

$$V_L = -0.23 - 0.85i, \qquad V_R = 0.03 + 0.60i,$$
$$T_L = 0.38 + 0.06i.\tag{44}$$

We define optimized rates for the NP contributions in the same way as has been done for the SM in Eq. (18). In Fig. 3, we plot the SM differential q^2 distributions of the
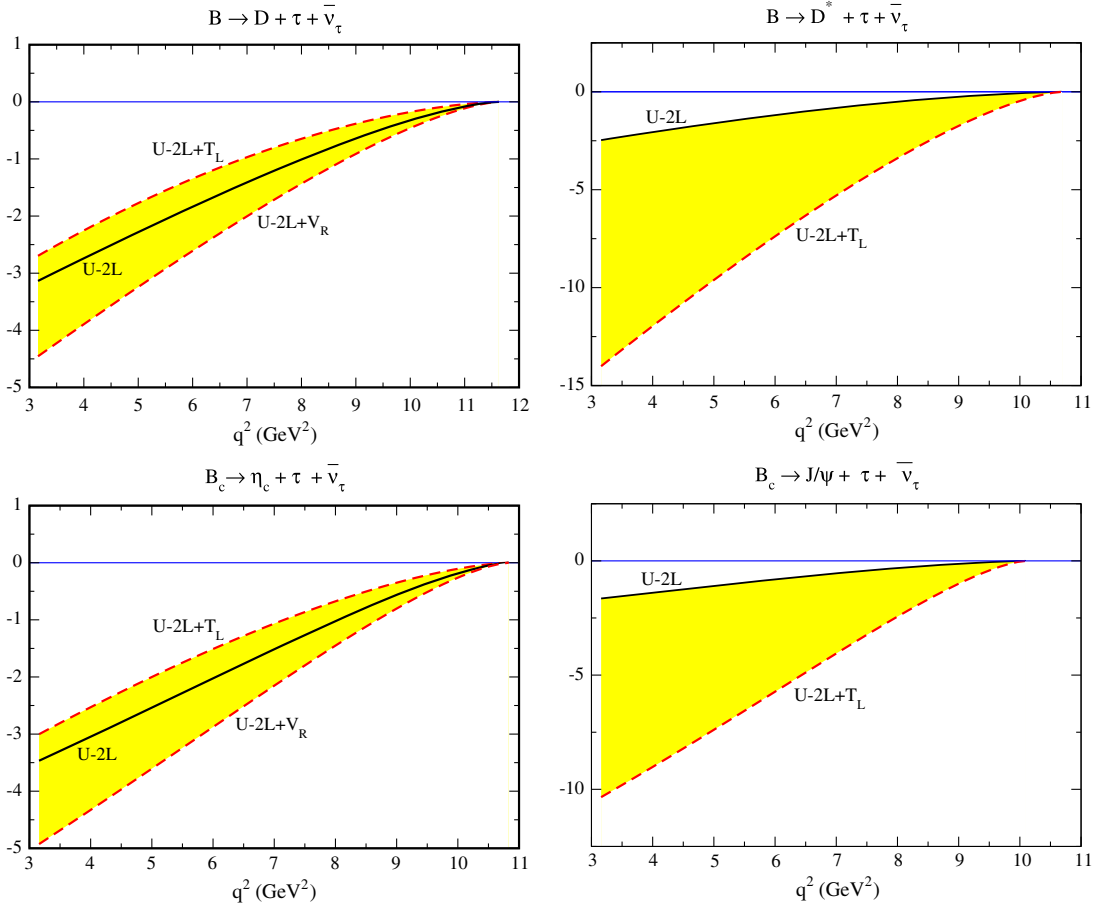
FIG. 3. $P \to P'(V)$ semileptonic transitions taking into account NP effects for the τ mode. The q^2 dependence of the optimized partial rates are shown in units of 10^{-15} GeV^{-1}. In the figures, we make use of the shorthand notation $U - 2L = d\Gamma^{\text{optd}}_{U-2L}/dq^2$.

optimized rates $d\Gamma^{\text{optd}}_{U-2L}/dq^2$ together with the corresponding (SM + NP) distributions for the τ mode. In general, there are four curves for each mode. To avoid oversaturation of the figures, we display the upper and lower curves only and the region between these two curves, colored in yellow. The $P \to P'$ optimized differential rates are enhanced by the NP V_L and V_R contributions and reduced by the NP tensor contribution T_L. For the $P \to V$ transitions, the enhancement due to the NP tensor contribution T_L is quite pronounced over the whole q^2 range.

The enormous size of the NP tensor contribution to the $P \to V$ transitions also shows up in Table III, where we list the integrated optimized rates and the τ/μ ratio of optimized branching fractions

$$R^{\text{optd}}_{U-2L}(\tau, \mu) = \frac{\Gamma^{\text{optd}}_{U-2L}(\text{SM} + \text{NP})}{\Gamma^{\text{optd}}_{U-2L}(\text{SM})}. \tag{45}$$

The deviations of the ratio of optimized branching fractions from the SM value of 1 is substantial and huge for the

TABLE III. Optimized $(U - 2L)$ rates in units of 10^{-14} GeV and rate ratios. NP effects are included in the τ mode only.

Obs	NP coupling	$B \to D\ell\nu_\ell$	$B_c \to \eta_c\ell\nu_\ell$	$B \to D^*\ell\nu_\ell$	$B_c \to J/\psi\ell\nu_\ell$
$\Gamma^{\text{optd}}_{U-2L}(\text{SM})$		-1.14	-1.21	-0.73	-0.89
$\Gamma^{\text{optd}}_{U-2L}(\text{SM} + \text{NP})$	V_L	-1.50	-1.59	-0.96	-0.64
	V_R	-1.62	-1.72	-0.94	-0.62
	T_L	-0.85	-0.93	-4.46	-3.32
$R^{\text{optd}}_{U-2L}(\tau, \mu)$	V_L	1.32	1.31	1.32	0.72
	V_R	1.42	1.42	1.29	0.70
	T_L	0.75	0.77	6.11	3.73

$P \rightarrow V$ transitions. One should be remindful of the fact that the NP optimized τ rates and thereby the ratio of branching fractions $B_{U-2L}^{\mathrm{optd}}(\tau, \mu)$ are form-factor dependent.

VII. SOME CONCLUDING REMARKS

As the authors of Ref. [22] have emphasized, it is important to also have a look at the (q^2, E_ℓ) distribution in semileptonic decays when testing lepton universality.

We briefly discuss the merits of using the (q^2, E_ℓ) distribution for form-factor-independent tests of lepton universality. One merit of (q^2, E_ℓ) distribution is obviously that $\cos\theta$ is a derived quantity, whereas the lepton energy can be directly measured.

The $(q^2, \cos\theta)$ distribution (3) can be transformed to the (q^2, E_ℓ) distribution by making use of the relation (8) between $\cos\theta$ and E_ℓ. One obtains

$$\frac{d\Gamma}{dq^2 dE_\ell} = \frac{1}{2S_1 + 1} \frac{3q^2}{|\vec{q}|^2} \frac{\Gamma_0}{m_1^7} \left(B_0(q^2, m_\ell) + B_1(q^2, m_\ell) \left(\frac{E_\ell}{m_1}\right) + B_2(q^2) \left(\frac{E_\ell^2}{m_1^2}\right) \right), \tag{46}$$

where the coefficients $B_0(q^2, m_\ell), B_1(q^2, m_\ell)$, and $B_2(q^2)$ are given, respectively, by

$$B_0(q^2, m_\ell) = \frac{1}{4}(q_0^2(1 + 2\delta_\ell)^2(\mathcal{H}_U - 2\mathcal{H}_L) + v|\vec{q}|^2(\mathcal{H}_U + 2\mathcal{H}_L + 2\delta_\ell(\mathcal{H}_U + 2\mathcal{H}_S))$$
$$+ 2q_0|\vec{q}|(1 + 2\delta_\ell)(\mathcal{H}_P + 4\delta_\ell\mathcal{H}_{SL})), \tag{47}$$

$$B_1(q^2, m_\ell) = -m_1(q_0(1 + 2\delta_\ell)(\mathcal{H}_U - 2\mathcal{H}_L) + |\vec{q}|(\mathcal{H}_P + 4\delta_\ell\mathcal{H}_{SL})), \tag{48}$$

$$B_2(q^2) = m_1^2(\mathcal{H}_U - 2\mathcal{H}_L). \tag{49}$$

The $(q^2, \cos\theta)$ distribution (46) can be seen to be well defined in the limit $|\vec{q}| \rightarrow 0$ since $\mathcal{H}_P, \mathcal{H}_{SL} \sim |\vec{q}|$, and $\mathcal{H}_U - 2\mathcal{H}_L \sim |\vec{q}|^2$ in all three classes of decays as discussed in Sec. IV.

In Fig. 4, we show the (q^2, E_ℓ) phase space boundaries of the three (e, μ, τ) modes of the semileptonic decay $\bar{B}^0 \rightarrow D^+ + \ell^- \bar{\nu}_\ell$. The phase space boundaries are determined by the curves [14,16]

$$q_\pm^2 = \frac{1}{a}(b \pm \sqrt{b^2 - ac}), \tag{50}$$

where

$$a = m_1^2 + m_\ell^2 - 2m_1 E_\ell,$$
$$b = m_1 E_\ell(m_1^2 - m_2^2 + m_\ell^2 - 2m_1 E_\ell) + m_\ell^2 m_2^2,$$
$$c = m_\ell^2((m_1^2 - m_2^2)^2 + m_\ell^2 m_1^2 - (m_1^2 - m_2^2)2m_1 E_\ell).$$

From the relation (8) linking $\cos\theta$ and E_ℓ, it is not difficult to see that the coefficients of the $\cos^2\theta$ and E_ℓ^2 terms are simply related. In particular, as Eq. (49) shows, the coefficient $B_2(q^2)$ of the quadratic E_ℓ^2 term is proportional to $\mathcal{H}_{U-2L}$ and, differing from the corresponding coefficient $\mathcal{H}_2$ of the $(q^2, \cos\theta)$ distribution, does not depend on the lepton mass. A gratifying feature of the (q^2, E_ℓ) analysis is the fact that the (model-dependent) ratio $A_2(q^2)/A_0(q^2, m_\ell)$ is quite large over the whole q^2 range [22].

Similar to Eq. (15), the second-order coefficient $B_2(q^2) = m_1^2\mathcal{H}_{U-2L}(q^2)$ can be projected from the distribution (46) by folding the distribution with the second-order Legendre polynomial expressed in terms of the lepton energy, i.e.,

$$P_2(\cos\theta(E_\ell)) = \frac{3}{2} \frac{1}{|\vec{q}|^2 v^2} \left(4E_\ell^2 - 4E_\ell q_0(1 + 2\delta_\ell) \right.$$
$$\left. + q_0^2(1 + 2\delta_\ell)^2 - \frac{1}{3}|\vec{q}|^2 v^2 \right). \tag{51}$$

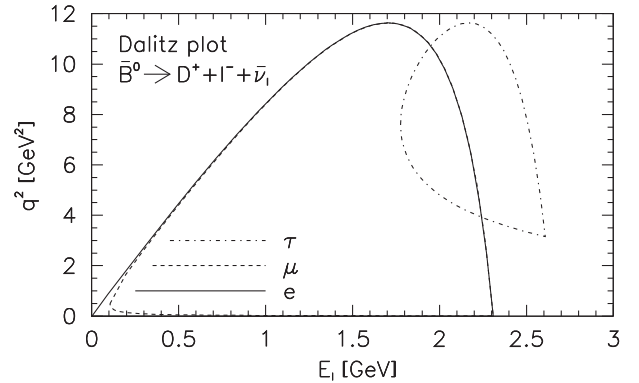The folding has to be done within the limits (E_ℓ^+, E_ℓ^-), where (see, e.g., Refs. [14,16])

FIG. 4. (q^2, E_ℓ) phase space for $\bar{B}^0 \rightarrow D^+ + \ell^- + \bar{\nu}_\ell$ for the three (e, μ, τ) modes.

$$E_\ell^\pm = \frac{1}{2}(q_0(1+2\delta_\ell) \pm |\vec{q}|v). \tag{52}$$

The zero- and first-order coefficients B_0 and B_1 in Eq. (46) are removed by the folding process, since

$$\int_{E_\ell-}^{E_\ell^+} dE_\ell P_2(\cos\theta(E_\ell)) = \int_{E_\ell-}^{E_\ell^+} E_\ell dE_\ell P_2(\cos\theta(E_\ell)) = 0, \tag{53}$$

as can be seen by direct calculation or by considering the orthogonality relations

$$\int_{E_\ell-}^{E_\ell^+} dE_\ell P_{0,1}(\cos\theta(E_\ell))P_2(\cos\theta(E_\ell)) = 0. \tag{54}$$

Similar to Eq. (15), one finds

$$\frac{d\Gamma_{U-2L}}{dq^2} = 10 \int_{E_\ell^-}^{E_\ell^+} dE_\ell \frac{d^2\Gamma}{dq^2 dE_\ell} P_2(\cos\theta(E_\ell))$$

$$= \frac{2}{2S_1+1} \frac{\Gamma_0|\vec{q}|q^2 v^3}{m_1^7} \mathcal{H}_{U-2L}(q^2). \tag{55}$$

To be sure, we have done the somewhat lengthy E_ℓ integration in Eq. (55) and confirmed the expected result on the rhs of Eq. (55). From here on, one would proceed as in Sec. III; i.e., one defines an optimized rate by dividing out the lepton-mass-dependent factor $v^3 = (1 - m_\ell^2/q^2)^3$. Differing from the $(q^2, \cos\theta)$ analysis discussed in the main text, the (q^2, E_ℓ) phase space is not rectangular, which means that the q^2 and E_ℓ integrations are not interchangeable. The projection of the relevant B_2 coefficient Eq. (55) has to be done for each q^2 value, or for each q^2 bin, before q^2 integration. In the τ mode, the range of E_ℓ becomes very small near threshold $q^2 = m_\tau^2$ and near the zero-recoil point $q^2 = (m_1 - m_2)^2$.

In summary, we have proposed a form-factor-independent test of lepton universality for semileptonic B meson, B_c meson, and Λ_b baryon decays by analyzing the twofold $(q^2, \cos\theta)$ decay distribution. We have defined optimized rates for the e, μ, τ modes, the ratios of which take the value of 1 in the SM, independently of form-factor effects. The form-factor-independent test involves a reduced phase space for the light lepton modes which will somewhat reduce the data sample for the light modes. The requisite angular analysis of the twofold $(q^2, \cos\theta)$ distribution will be quite challenging from the experimental point of view. We have discussed new physics effects for the τ mode, the inclusion of which will lead to large aberrations from the SM value of 1 for the ratio of the optimized rates. As a by-line, we have also included a discussion of the (q^2, E_ℓ) decay distribution as a possible candidate for form-factor-independent tests of lepton universality.

We conclude with two remarks. We have made a wide survey of polarization observables in semileptonic b hadron decays to find an observable with the requisite property that the helicity-flip dependence factors out of the observable. In fact, in semileptonic polarized Λ_b decay, one can identify the observable $v(\mathcal{H}_P - 2\mathcal{H}_{L_-})$ which possesses the desired property [16,19]. All in all, we are looking forward to experimental tests of lepton universality using the optimized branching ratios proposed in this paper.

[1] J. Lees *et al.* (*BABAR* Collaboration), Phys. Rev. Lett. **109**, 101802 (2012).

[2] J. P. Lees *et al.* (*BABAR* Collaboration), Phys. Rev. D **88**, 072012 (2013).

[3] A. Bozek *et al.* (Belle Collaboration), Phys. Rev. D **82**, 072005 (2010).

[4] M. Huschle *et al.* (Belle Collaboration), Phys. Rev. D **92**, 072014 (2015).

[5] Y. Sato *et al.* (Belle Collaboration), Phys. Rev. D **94**, 072007 (2016).

[6] S. Hirose *et al.* (Belle Collaboration), Phys. Rev. Lett. **118**, 211801 (2017).

[7] R. Aaij *et al.* (LHCb Collaboration), Phys. Rev. Lett. **115**, 111803 (2015); **115**, 159901(E) (2015).

[8] Y. S. Amhis *et al.* (HFAG Collaboration), arXiv:1909.12524.

[9] F. U. Bernlochner, M. F. Sevilla, D. J. Robinson, and G. Wormser, arXiv:2101.08326.

[10] R. Barbieri, arXiv:2103.15635.

[11] K. Cheung, Z. R. Huang, H. D. Li, C. D. Lü, Y. N. Mao, and R. Y. Tang, Nucl. Phys. **B965**, 115354 (2021).

[12] T. D. Cohen, H. Lamm, and R. F. Lebed, Phys. Rev. D **100**, 094503 (2019).

[13] J. G. Körner and G. A. Schuler, Phys. Lett. B **231**, 306 (1989).

[14] J. G. Körner and G. A. Schuler, Z. Phys. C **46**, 93 (1990).

[15] P. Bialas, J. G. Körner, M. Krämer, and K. Zalewski, Z. Phys. C **57**, 115 (1993).

[16] A. Kadeer, J. G. Körner, and U. Moosbrugger, Eur. Phys. J. C **59**, 27 (2009).

[17] T. Gutsche, M. A. Ivanov, J. G. Körner, V. E. Lyubovitskij, P. Santorelli, and N. Habyl, Phys. Rev. D **91**, 074001 (2015); **91**, 119907(E) (2015).

[18] M. A. Ivanov, J. G. Körner, and C. T. Tran, Phys. Rev. D **92**, 114022 (2015).

[19] S. Groote, J. G. Körner, and B. Melić, Eur. Phys. J. C **79**, 948 (2019).

[20] E. Di Salvo, F. Fontanelli, and Z. J. Ajaltouni, Int. J. Mod. Phys. A **33**, 1850169 (2018).

[21] M. Fischer, S. Groote, J. G. Körner, and M. C. Mauser, Phys. Rev. D **65**, 054036 (2002).

[22] N. Penalva, E. Hernández, and J. Nieves, Phys. Rev. D **100**, 113007 (2019).

[23] N. Penalva, E. Hernández, and J. Nieves, Phys. Rev. D **101** (2020) 113004.

[24] N. Penalva, E. Hernández, and J. Nieves, Phys. Rev. D **102**, 096016 (2020).

[25] C. S. Kim, S. C. Park, and D. Sahoo, Phys. Rev. D **100**, 015005 (2019).

[26] M. Freytsis, Z. Ligeti, and J. T. Ruderman, Phys. Rev. D **92**, 054018 (2015).

[27] F. U. Bernlochner and Z. Ligeti, Phys. Rev. D **95**, 014022 (2017).

[28] G. Isidori and O. Sumensari, Eur. Phys. J. C **80**, 1078 (2020).

[29] W. Detmold, C. Lehner, and S. Meinel, Phys. Rev. D **92**, 034503 (2015).

[30] A. Datta, S. Kamali, S. Meinel, and A. Rashed, J. High Energy Phys. 08 (2017) 131.

[31] S. Meinel and G. Rendon, arXiv:2103.08775.

[32] J. A. Bailey *et al.* (Fermilab Lattice and MILC Collaborations), Phys. Rev. D **89**, 114504 (2014).

[33] J. A. Bailey *et al.* (MILC Collaboration), Phys. Rev. D **92**, 034506 (2015).

[34] H. Na, C. M. Bouchard, G. P. Lepage, C. Monahan, and J. Shigemitsu (HPQCD Collaboration), Phys. Rev. D **92**, 054510 (2015); **93**, 119906(E) (2016).

[35] D. Bigi and P. Gambino, Phys. Rev. D **94**, 094008 (2016).

[36] F. U. Bernlochner, Z. Ligeti, M. Papucci, and D. J. Robinson, Phys. Rev. D **95**, 115008 (2017); **97**, 059902 (E) (2018).

[37] P. Gambino, M. Jung, and S. Schacht, Phys. Lett. B **795**, 386 (2019).

[38] M. Bordone, M. Jung, and D. van Dyk, Eur. Phys. J. C **80**, 74 (2020).

[39] C. T. Tran, M. A. Ivanov, J. G. Körner, and P. Santorelli, Phys. Rev. D **97**, 054014 (2018).

[40] P. A. Zyla *et al.* (Particle Data Group), Prog. Theor. Exp. Phys. **2020**, 083C01 (2020).

[41] G. Ciezarek, M. F. Sevilla, B. Hamilton, R. Kowalewski, T. Kuhr, V. Lüth, and Y. Sato, Nature (London) **546**, 227 (2017).

[42] D. Becirevic, S. Fajfer, I. Nisandzic, and A. Tayduganov, Nucl. Phys. **B946**, 114707 (2019).

[43] M. A. Ivanov, J. G. Körner, and C. T. Tran, Phys. Rev. D **94**, 094028 (2016).

[44] C. T. Tran, M. A. Ivanov, and J. G. Körner, arXiv:1702.06910.